HiSST: 2nd International Conference on
High-Speed Vehicle Science Technology
11–15 September 2022, Bruges, Belgium

A Multi-fidelity Simulation Method for Hypersonic Airbreathing Propulsion System

Jun Liu[1],Huacheng Yuan[2],Jinsheng Zhang[3], Zheng Kuang[4]

Abstract

As the hypersonic vehicle is highly integrated, a multi-fidelity simulation method based on commercial solver is developed to save the simulation time for this vehicle and its propulsion system. This method is characterized with high-level fidelity numerical analysis of external flow and low-level fidelity numerical analysis of internal flow. The external flow of propulsion system are solved by RANS equations. The internal flow is modeled by quasi-one dimensional equation. The interaction between external and interflow is governed by the CFD solver through user-defined function. The static pressure distribution acquired from multi-fidelity simulation method agrees well with the experimental data, indicating that this simulation method can be used to study the flow physics in hypersonic propulsion system at a reasonable cost. The results from design point indicate that the horizontal force increases with fuel equivalence ratio and the thrust balance is realized at φ=0.35. The positive net thrust is maintained throughout the flight regime from Ma 4 to Ma7 whether the combustor operates in ramjet or scramjet mode.

Keywords: *hypersonic air-breathing propulsion system, external and internal flow, quasi-one dimensional model, multi-fidelity simulation method*

Nomenclature

Latin
A – Area
a – Sonic speed
c – Coefficient
e – Internal energy
f – Friction coefficient
h – Height
Ma – Mach number
p – Static pressure
Pt – Total pressure
T – Static temperature
t – Time
Tt – Total temperature
U – Velocity
x – Horizontal coordinate
y – Vertical coordinate
Greek
ρ – Density
φ – Fuel equivalence ratio
Subscripts
0 – Free-stream station
3 – Combustor entrance station
4 – Combustor exit station
10 – Nozzle exit station
c – Combustor
f – Fuel

[1] *Nanjing University of Aeronautics and Astronautics, Nanjing 210016, People's Republic of China E-mail:liujunnever @nuaa. edu.cn*
[2] *Nanjing University of Aeronautics and Astronautics, Nanjing 210016, People's Republic of China E-mail: yuanhuacheng@nuaa. edu.cn*
[3] *Nanjing University of Aeronautics and Astronautics, Nanjing 210016, People's Republic of China*
[4] *Nanjing University of Aeronautics and Astronautics, Nanjing 210016, People's Republic of China*

1. Introduction

As we know, scramjet propulsion system is critical for hypersonic cruise vehicle. To reduce the external drag and improve lift-to-drag ratio of hypersonic cruise vehicle[1,2], the scramjet propulsion system which consists of forebody/inlet[3], combustor[4], nozzle/afterbody[5] is integrated with hypersonic cruise vehicle. Although three dimension simulations will give more accurate and details of the physical flows inside the propulsion system, it is time consuming. Thus, in order to reduce the simulation time and acquire preliminary result of hypersonic cruise vehicle and propulsion system in the design process. Quasi-one dimensional method[6-8] or multi-fidelity simulation method[9] are used. The external flow field is simulated by CFD code and the internal flow field is solved by quasi-one dimensional model.

There are mainly two methods to calculate the flow properties along the combustor. The first one is Heiser and Prattl approach [2], which uses space-marching method to solve the governing equation. This governing equation takes combustor area variation and total temperature distribution into account. Smart[10] developes a Mach number distribution ordinary difference equation (ODE) incorporates wall frection. This normalized ODE was based on isentropic flow equations derivated by Shapiro [11]. This method is difficult to deal with thermal choke where Mach number of flow is unity. To solve the ODE, the core flow area has to be prescribed.[6] The other one is the quasi-one dimensional unsteady method proposed by Bussing[12], which was developed from computational fluid dynamics equations and uses time-marching method to solve the governing equations. Liu et al.[13] used this method to calculate the unsteady quasi-one dimensional combustor with skin friction, heat dissipation and fuel mixture model. Wang [14] took into account the finite-rate chemical reaction in the combustor model. Compared with the experimental data, Billing[15] and Jiang et al. [16] considered the pre-combustion shock train in this model and developed the coupling algorithm between isolator and combustor suitable for dual-mode scramjet.

Multi-fidelity simulation method of air-breathing propulsion system has also been investigated. Kim et al.[17] studied the flow field around a N2B Hybrid Wing Body Configuration. The external flow was simulated by CFD code and propulsion system was provided by NPSS thermodynamic engine cycle model. Their results revealed complex flow physics from the integrated airframe-propulsion system. Vijayakumar et al. [18] implemented quasi-one dimensional combustor model into the Numerical Propulsion System Simulation (NPSS) and simulated the flowfield coupled with FLUENT code. In their work, the flow simulation of compression system was carried out by FLUENT solver at off-design cases. The coupling of NPSS and FLUENT was process coupling method.[18] Complex flow physics through a dual-mode scramjet engine compression system operating from Ma 3.5 to 6.0 has been studied. Their work demonstrates the importance of multifidelity and component-integrated analysis. Due to the lack of flame blowout prediction capabilities developed by Vijayakumar et al. [18] and Vu and Wilson[6], Connolly et al.[19] implemented a generalized DMSJ combustors model into NPSS which can identified four operation modes including unstart, ramjet, scramjet and blowout of the combustor. Based on NPSS, they built a turbine-based combined cycle, which can operate from take-off to above Mach 5. In their work, mode transition from turbomachinery to DMSJ operation is simulated successfully.

In this paper, we developed a multi-fidelity simulation method based on a commercial flow solver. The external flow fields of the hypersonic vehicle are calculate using the commercial flow solver, while the internal flow of the combustor is calculated using quasi-one dimensional model based on C programming language. Firstly, the methodology for this multi-fidelity simulation is introduced. The validation of quasi-one dimensional combustor model is then carried out based on the experiment tests. Finally, the external and internal flow fields at design and off-design points of hypersonic cruise vehicle are illustrated.

2. Multi-fidelity simulation method

2.1. Computational fluid dynamics solver

A two-dimension steady state, implicit, density based, ANSYS® FLUENT 14.5 solver was used for solving the fluid flow. The Reynolds Averaged Navier-Stokes (RANS) equations were solved for the inlet and nozzle components of hypersonic propulsion systems. The mass, momentum and energy conservation equations are shown in Eq.1-3.

Mass conservation equation:

$$\frac{\partial \rho}{\partial t} + \nabla \cdot (\rho \boldsymbol{U}) = 0 \tag{1}$$

Momentum conservation equation:

$$\frac{\partial}{\partial t}(\rho \boldsymbol{U}) + \nabla \cdot (\rho \boldsymbol{U}\boldsymbol{U}) = -\nabla p + \nabla \cdot \tau + \rho \boldsymbol{g} \tag{2}$$

where p is the static pressure, τ is the stress tensor (described below), and $\rho \boldsymbol{g}$ is the gravitational body force.

Energy conservation equation:

$$\frac{\partial}{\partial t}\left[\rho\left(e + \frac{U^2}{2}\right)\right] + \nabla \cdot \left[\rho\left(e + \frac{U^2}{2}\right)\boldsymbol{U}\right] = -p\nabla \cdot \boldsymbol{U} + \nabla \cdot (\lambda \nabla T) + \Phi + S_h \tag{3}$$

where λ is effective conductivity, Φ is dissipation function and S_h is volumetric heat sources.

These equations are discretized with a finite volume method. The implicit solution formulation is selected. Roe flux-difference splitting (Roe-FDS) scheme is used to discretized the convective fluxes. The viscid flux is discretized based on second order central difference scheme. The one-equation S-A equation is used to model the turbulent flow. The fluid is treated as compressible ideal gas. The molecular viscosity of the gas is calculated using Sutherland's law with three coefficients defined as:

$$\mu = \mu_0 \left(\frac{T}{T_0}\right)^{3/2} \frac{T_0 + S}{T + S} \tag{4}$$

where reference viscosity μ_0 and reference temperature T_0 are $1.716\times10^{-5}\mathrm{kg/ms^{-1}}$ and $273.11\mathrm{K}$, respectively. Effective temperature S is 110.56K.

2.2. Quasi-one dimensional flow model

The combustor component is modelled by quasi-one dimensional flow conservation Eq. 5, which account for mass addition, area variable, wall friction and heat release. These factors are included in the source term **J**.

$$\frac{\partial \boldsymbol{U}}{\partial t} + \frac{\partial \boldsymbol{F}}{\partial x} = \boldsymbol{J} \tag{5}$$

where **U** is the solution vector, **F** and **J** are the flux vector and the source term defined as follow:

$$\boldsymbol{U} = \begin{bmatrix} \rho A \\ \rho A U \\ \rho(e + U^2/2)A \end{bmatrix}, \boldsymbol{F} = \begin{bmatrix} \rho A U \\ \rho A U^2 + pA \\ \rho(e + U^2/2)AU + pAU \end{bmatrix}, \boldsymbol{J} = \begin{bmatrix} \dfrac{d\dot{m}_f}{dx} \\ p\dfrac{\partial A}{\partial x} - \dfrac{\rho U^2}{2} f \cdot C_{\mathrm{wet}} \\ \dfrac{d\dot{Q}}{dx} \end{bmatrix} \tag{6}$$

where $d\dot{m}_f$ is fuel mass flow rate, f is combustor wall friction coefficient ranging from 0.003 to 0.005 and set to 0.003 in this paper, C_{wet} is the combustor wet perimeter, $\mathrm{d}\dot{Q}$ is cumulative heat release. The

cumulative heat release distribution schedule is determined by a power law relationship using the non-dimensional length along the combustor [20]:

$$Q(x) = Q_{\max}\left(\frac{x}{L_c}\right)^{\frac{1}{3}} \tag{7}$$

where $Q_{max} = f_{st}H_{prop}$, f_{st} is the stoichiometric ratio, $H_{prop}$is the heat value and L_c is the length of combustor.

The quasi-one dimensional conservation equations are solved by MacCormack numerical scheme [21]. It is a two-step, second order accurate in both time and space, explicit finite difference method. The forward difference scheme is used to calculate the spatial discretization at the predictor step:

$$\overline{\boldsymbol{U}}_i^n = \boldsymbol{U}_i^n - \frac{\Delta t}{\Delta x}\left(\boldsymbol{F}_{i+1}^n - \boldsymbol{F}_i^n\right) + \Delta t \boldsymbol{J}_i^n \tag{8}$$

The backward difference scheme is used at the corrector step:

$$\boldsymbol{U}_i^{n+1} = \frac{1}{2}\left[\boldsymbol{U}_i^n + \overline{\boldsymbol{U}}_i^n - \frac{\Delta t}{\Delta x}\left(\boldsymbol{F}_i^{n+1} - \boldsymbol{F}_{i-1}^{n+1}\right) + \Delta t \boldsymbol{J}_i^{n+1}\right] \tag{9}$$

where supscript n represents time, t=nΔt, subscript i refers to the spatial grid point x_i. The time step is determined based on the numerical stability equation:

$$\Delta t \le \mathrm{CFL}\frac{\Delta x}{V + a} \tag{10}$$

CFL number must be less than or equal to 1.0 for MacCormack scheme be stable.

To damp out numerical oscillations in the vicinity of large gradients, artificial viscosity is introduced in MacCormack's method. The artificial viscosity applied to the conservation equations is define as:

$$\boldsymbol{S}_i^n = Nu\frac{\left|p_{i+1}^n - 2p_i^n + p_{i-1}^n\right|}{p_{i+1}^n + 2p_i^n + p_{i-1}^n}\left(\boldsymbol{U}_{i+1}^n - 2\boldsymbol{U}_i^n + \boldsymbol{U}_{i-1}^n\right) \tag{11}$$

where Nu is an adjustable viscosity-like constant. The value of Nu varies from 0.01 to 0.3 and we choose Nu =0.1 based on the accuracy of final solution.

To solve the quasi-one-dimensional equations, the upstream and downstream boundary conditions need to be specified. There are two types of flow at these two boundaries depending on the direction of three characterisitcs (U+a, U-a, a). For supersonic condition, all three characteristics point into upstream boundary and out of downstream boundary. For subsonic condition, one characteristics (U-a) points out of upstream and in from the downstream boundary.

The combustor may operate in ramjet or scramjet mode, therefore the upstream boundary condition of combustor is subsonic or supersonic upstream boundary conditions. For supersonic conditions, the values of three conservation variables were calculated from the upstream total pressure, total temperature and Mach number. For subsonic conditions, the static pressure was determined from the combustor model. The first two conservation variables U_1 and U_2 were extrapolated from the upstream boundary and used together with specific static pressure to calculate U_3.

In this paper, only supersonic downstream boundary conditions were consider. The three conservation variable were extrapolated from interior points, which is defined as followed:

$$\boldsymbol{U}_{i\ \mathrm{exit}} = 2\boldsymbol{U}_{i\ \mathrm{exit\text{-}1}} - \boldsymbol{U}_{i\ \mathrm{exit\text{-}2}} \tag{12}$$

2.3. Coupling of quasi-one dimensional model and CFD codes

The coupling procedure between combustor and inlet/nozzle components is illustrated in this section. The schematic diagram of hypersonic vehicle is shown in Fig. 1. There are three main components for hypersonic airbreathing propulsion system, including forebody/inlet, combustor and nozzle/afterbody.

As the inlet and nozzle components are solved with two dimensional RANS equations. A mass-weighted average is used to calculate the flow quantities at the interfaces[22], which is defined by:

$$\bar{\phi} = \frac{\int \rho \phi dA}{\int \rho dA} \tag{13}$$

where ρ is the density, ϕ is any conserved quantity to be one dimensionalized, A is the area over which the average is being performed and $\bar{\phi}$ represents flow quantity after mass-weighted average.

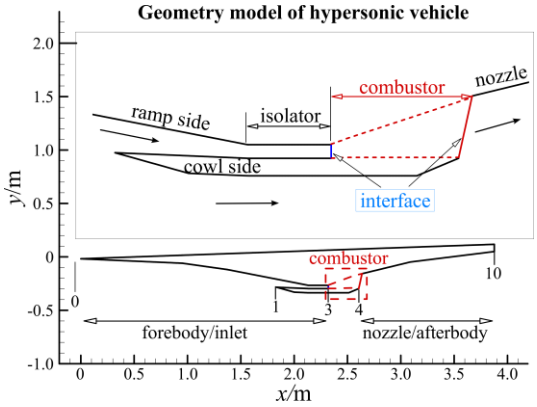

Fig 1. Schematic diagram of hypersonic vehicle

The coupling procedure of this multi-fidelity simulation is illustrated in Fig. 2.

(1) Solve 2D RANS equations and acquire the initial external flow fields.

(2) Calculate the mass-weighted average quantities at the interfaces.

(3) Solve quasi-one dimensional equation based on the upstream and downstream boundary conditions of combustor.

(4) Update the values at the interfaces and re-computate external flow fields.

(5) If iteration converges, then stop; otherwise return to step (1).

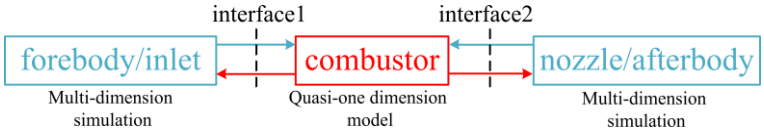

Fig 2. Coupling procedure of multi-fidelity simulation method

Based on the multi-fidelity simulation method introduced previously, the flow field of hypersonic vehicle with propulsion system is investigated. The schematic diagram of this vehicle is shown in Fig. 1 and detail dimensions of hypersonic propulsion system are shown in Table 1. As mention previously, inlet and nozzle are solved with CFD solver and the mesh and boundary conditions are shown in Fig. 3. ICEM software is used to generate the mesh and local refinement is conducted for regions with significant velocity gradient such as in the vicinity of shock waves and wall. The inflow is set as pressure far-field boundary condition. The outflow is set as pressure outlet. The entrance and exit of combustor are set as pressure outlet and pressure inlet boundary conditions, respectively. The quasi-one dimensional combustor model is implement into FLUENT solver by user-defined function (UDF).

Table 1. Geometry properties of hypersonic vehicle

Properties	values	Properties	values
inlet length(m)	2.13	Capture height(m)	0.27
isolator length(m)	0.187	Throat height(m)	0.03
combustor length(m)	0.32	Total contraction ratio	8.76
nozzle length(m)	0.124	Combustor area ratio	4.63
ramp angles	2.5°, 5.5° , 3°,	Nozzle expansion ratio	2.49

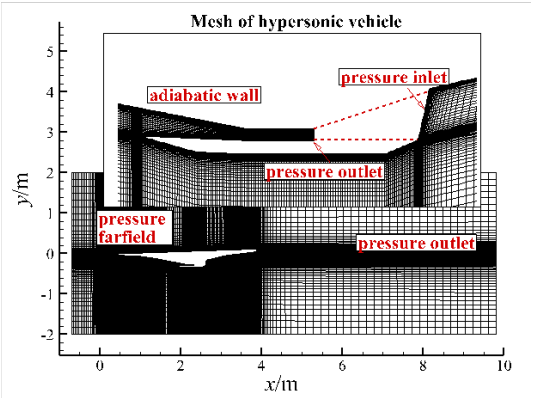

Fig 3. Mesh and boundary conditions of hypersonic vehicle

2.4. Validation

The quasi-one dimensional simulation method adopted in this paper is verified by the combustor experiment tests from University of Virginia[23]. The schematic of experimental model is shown in Fig.4. This model is installed on the direct connected facility consists of Laval nozzle, isolator, combustor and diffuser. The combustor can be split into two sections, each of which is made up of rectangular tubes with constant cross-section and single expansion diffuser. Hydrogen is chosed as the fuel and injected through a 10° ramp. The experimental model is non-dimensional with respect to the injector ramp height (h). During the test, total temperature at the isolator entrance is 1160 K, total pressure is 330 kPa, Mach number is 2.03 and fuel equivalence ratio φ varies from 0 to 0.31. Test results with fuel equivalence ratio of 0 and 0.21 are used to verify the simulation method developed in this paper.

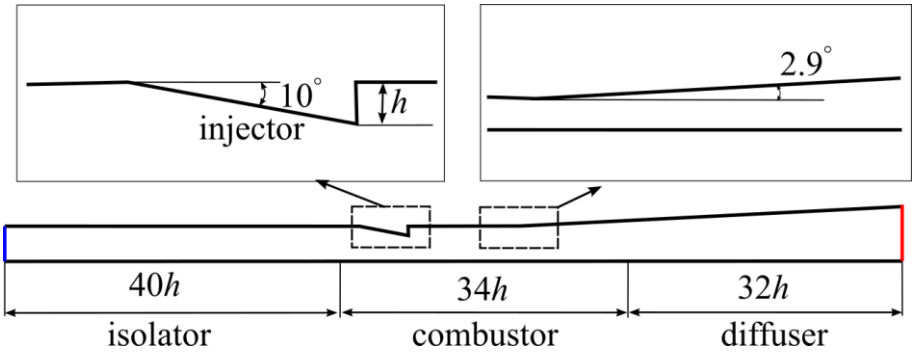

Fig 4. The schematic of experimental model

The static pressure distribution along the flowpath between experiment tests and multi-fidelity simulation at different fuel equivalence ratios are shown in Fig. 5. The close symbols represent the experimental tests and solid lines represent the simulation results. As shown in the figure the pressure distribution from multi-fidelity simulations agree well with the experimental tests. There is a pressure fluctuation at the entrance of the combustor as the combustor is power off (φ=0). It is due to the geometry of the injector is not considered during multi-fidelity simulations. In the test, the inflow is supersonic and oblique shock is induced from the injector ramp. As the combustor operates at φ=0.21, the results agree well with tests including starting location of the shock train[24] and the maximum static pressure along the internal flow path. Therefore, the multi-fidelity simulations method introduced above is accurate enough for further investigation.

Table 2. Flow Properties at the entrance of combustor after mass-weighted average

φ	Ma	P（kPa）	T(K)	Pt（kPa）	Tt(K)
0	1.81	49.09	617.1	298.93	1020.0
0.21	0.9871	129.75	848.75	257.62	1020.0

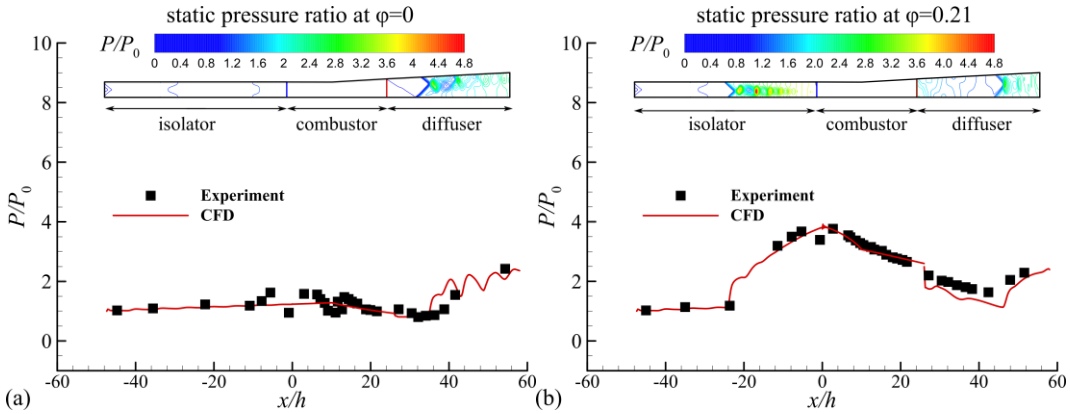

Fig 5. Multi-fidelity simulations compared to wind tunnel tests

3. Results

3.1. Design point

Based on the multi-fidelity simulation method presented previously, the flow field of an integrated hypersonic vehicle is investigated. In this section, we are going to discuss the design point results from the simulation.

Mach number contour and static pressure ratio along the ramp side of hypersonic vehicle at different fuel equivalence ratios are shown in Fig. 6. In Fig. 6(c), the blue solid line with triangle symbols represents combustor power off mode and the red solid line with rectangle symbols represents the fuel equivalence ratio at 0.60. The static pressure distribution at these two fuel equivalence ratios remains the same until the isolator. As the combustor power off shown in Fig. 6(a), there is no shock train in the isolator and the oblique shock waves reflect between ramp side and cowl side of the vehicle which causes the static pressure fluctuation in Fig.6(c). As the combustor power on, oblique shock train forms in the isolator as shown in Fig.6 (b) due to high backpressure in the combustor. The static pressure rises sharply and part of the flow speed decelerates to the subsonic and then flow into the combustor.

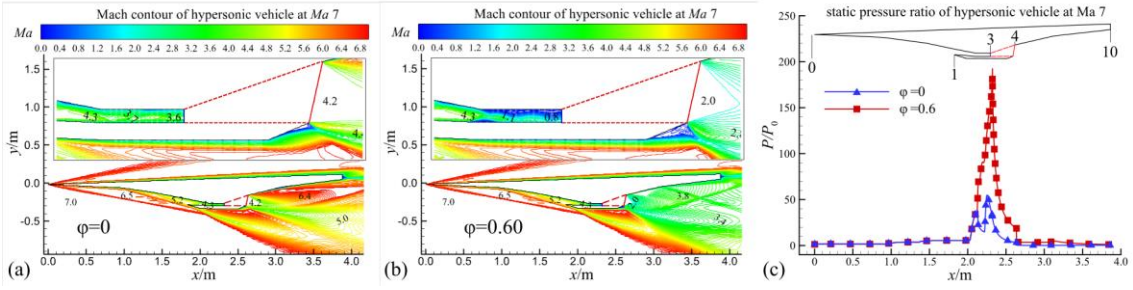

Fig 6. Mach contour and static pressure of hypersonic vehicle at *Ma* 7

The profiles of flow quantities passed on to the quasi-one dimensional combustor model are shown in Fig. 7. The total temperature, total pressure, Mach number and mass flow rate from CFD solver are mass-weighted average and then pass onto the combustor. The flow quantities along the combustor are presented in Fig. 8, as the combustor power on and operates at fuel equivalence ratio 0.60. As shown in Fig. 8, a thermal choke form at axis position x=2.35 m. The Mach number decreases from the entrance of combustor until the thermal choke and then increase gradually due to the diffusing of the combustor flowpath. The temperature increases significantly at the beginning of the combustor and then increases gradually until the end of the combustor.

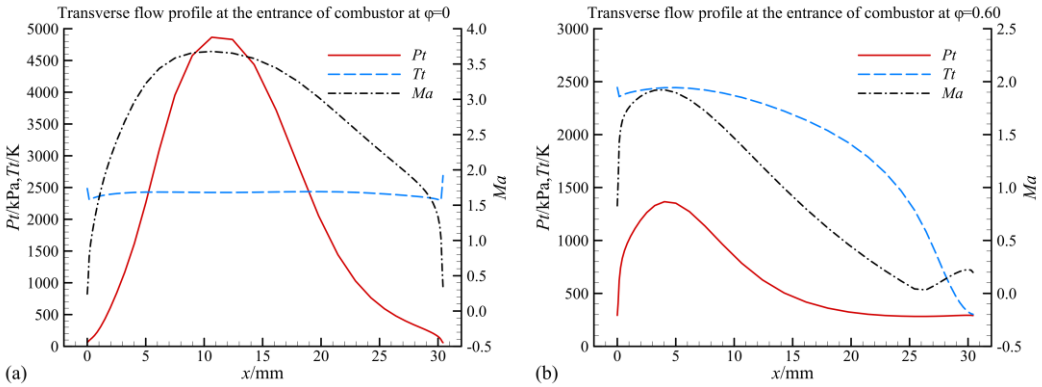

Fig 7. Transverse Flow Profile at the entrance of the combustor

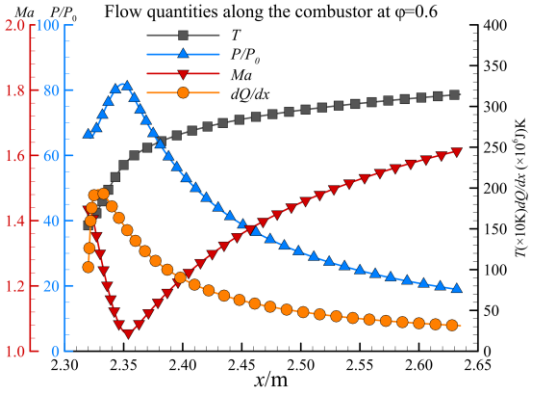

Fig 8. Flow quantities along the combustor at φ=0.60

As shown in Fig. 8, flow quantities including temperature, static pressure ratio, Mach number, heat release profile along the combustor are discussed. We are going to discuss flow property at different fuel equivalence ratios. Mach number along the combustor at fuel equivalence ratio from 0 to 0.6 are shown in Fig. 9. As the combustor power off, the Mach number along the flowpath increases gradually due to the divergence of combustor chamber. Mach number at the end of combustor decreases from 4.0 to 1.2 with fuel equivalence ratio. The combustor operates in scramjet mode when the fuel equivalence ratio is less than 0.5. As the fuel equivalence ratio is increased further, a thermal choke occurs and the combustor operation mode progressively shifts from scramjet to ramjet.

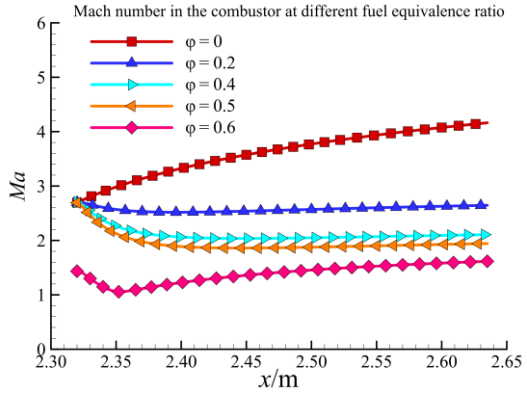

Fig 9. Mach number along the combustor at fuel equivalence ratio from 0 to 0.6

According to the external and internal flow fields calculate previously, the flow properties at different stations of hypersonic vehicle are summarized in Table 3. The horizontal and vertical force coefficients at fuel equivalence ratios ranging from 0 to 0.60 are shown in Fig.10, where horizontal force and vertical force coefficients are defined as:

$$c_x = \frac{F_x}{1/2\rho U^2 A_0}, c_y = \frac{F_y}{1/2\rho U^2 A_0} \tag{14}$$

The horizontal and vertical forces containing pressure and skin friction terms are integrated from the external and internal surfaces of the hypersonic vehicle. The horizontal force coefficient is positive at φ=0, which represents the drag as the combustor power off. The horizontal force coefficient decreasing with fuel equivalence ratio linearly until φ=0.5. The horizontal force coefficient is zero at φ=0.35, which indicates the thrust produce by the propulsion system is equal to the drag of the vehicle at this fuel equivalence ratio. Beyond this point, the thrust is greater than the drag. The deflection of horizontal force coefficient is due to the operation condition of the combustor switch from scramjet to ramjet mode, which can be found from Fig. 9. The vertical force coefficient which indicates the lift of the hypersonic vehicle increases with fuel equivalence ratio. Corresponding to horizontal force coefficient, it increases linearly as the combustor operates in scramjet mode.

Table 3. Station Flow Properties at design point

φ	station	Ma	P（kPa）	T(K)	Pt（kPa）	Tt(K)
0	0	7.0	1.6	224.5	6736.4	2419.4
	3	3.12	50.9	856.2	2908.5	2419.4
	4	4.16	5.40	534.2	1019.3	2382.1
	10	6.09	0.60	293.4	931.5	2382.1
0.6	3	1.37	233.9	1548.9	872.5	2419.4
	4	1.97	30.1	2022.9	223.2	3581.2
	10	3.47	2.8	1058.8	202.4	3578.1

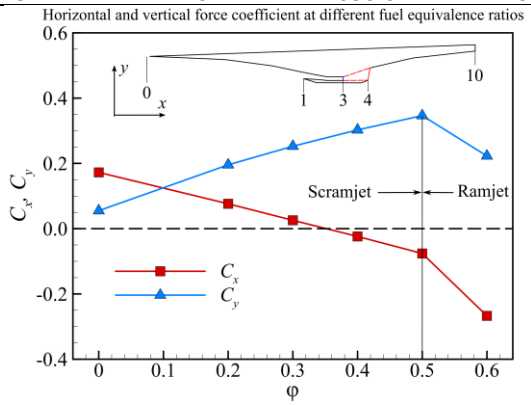

Fig 10. Horizontal and vertical force coefficients at fuel equivalence ratio from 0 to 0.6

Off-design points

The flow fields and quantities at the design point of hypersonic vehicle are investigated above, then we are going to discuss the flow fields and quantities at the off-design points at this section. The flow fields from Ma 4 to 6 are presented in Fig. 11. According to the Mach number at the exit of isolator, we can divide the operation of combustor into ramjet and scramjet mode. The Mach number at the exit of isolator is lower than 1.0 from Ma 4.0 to 5.5, indicating that the combustor is operating in ramjet mode. As the inflow Mach number increases to Ma 6, the operation mode of combustor switch to scramjet mode.

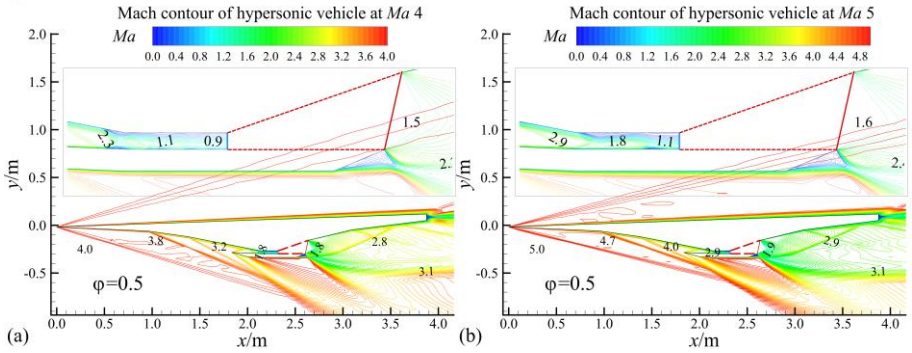

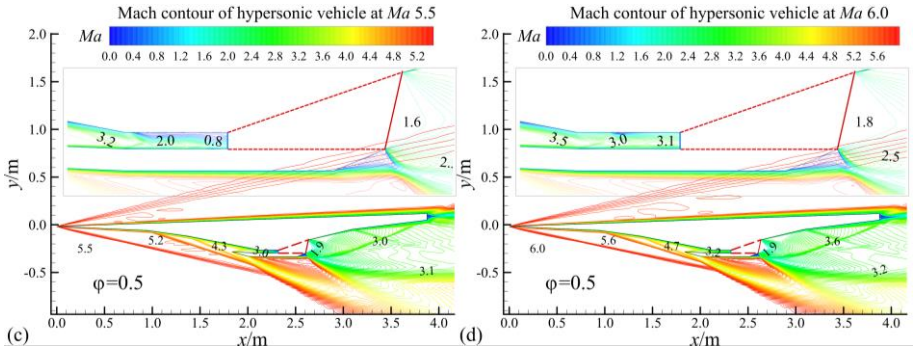

Fig 11. Mach contour at off-design point from Mach 4 to 6

The static pressure ratio of ramjet and scramjet mode is shown in Fig. 12. The static pressure rises with oblique shocks from ramps. Significant pressure rises in the inlet isolator due to shock trains. The shock train structure is obviously in the ramjet mode. As the inflow increases up to Ma 6, Mach number at the exit of isolator is supersonic and the combustor operates in scramjet mode.

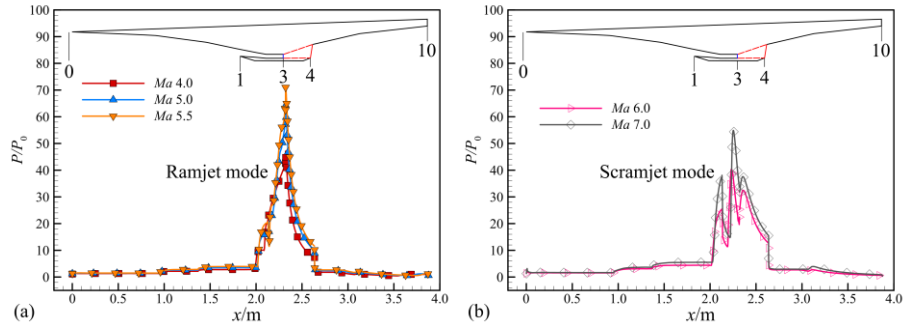

Fig 12. Static pressure ratio at off-design points from Mach 4 to 6

After the analysis of flow field and static pressure ratio distribution we gain some basic knowledge about flow physics at off-design points. Now we are going to study more details in the combustor. The temperature and Mach number along the combustor at the off-design points are shown in Fig. 13. In this figure, the solid symbols represent the ramjet mode and the open symbols represent the scramjet mode. During the ramjet mode, the temperature increases significantly at the beginning of the combustor and then increases mildly until the end of the combustor. The maximum temperature increases with inflow Mach number. As for the Mach number, it decreases first and then increases until the end of the combustor. During the scramjet mode, the temperature distribution law is similar to the ramjet mode by the temperature at the entrance of the combustor is lower than ramjet mode. As for the Mach number at scramjet mode, it decreases with the significant heat release at the beginning of the combustor and then remains almost constant due to area diffusing and heat release until the end of the combustor.

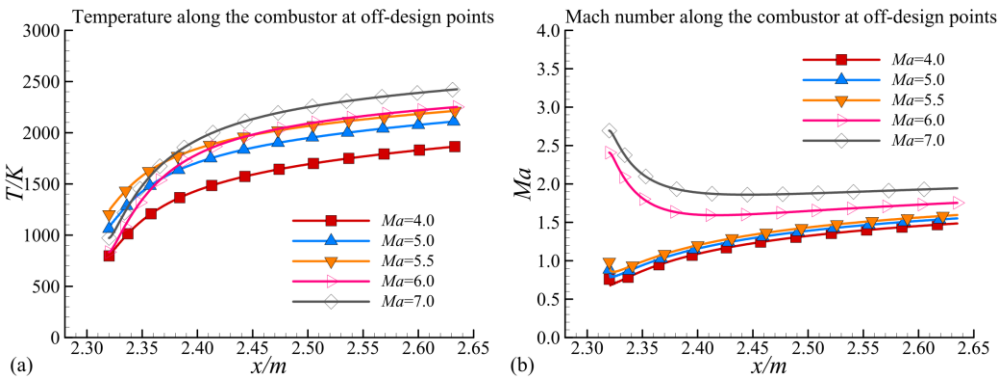

Fig 13. Temperature and Mach number along the combustor at off-design points from Mach 4 to 6

According to the external and internal flow fields calculate previously, the horizontal and vertical force coefficients at inflow Mach number from 4 to 7 are shown in Fig.14. The horizontal and vertical forces

including pressure and viscous terms are integrated from the external and internal surfaces of the hypersonic vehicle. The horizontal force coefficient is negative with this Mach number range, which indicates that the propulsion system can produce net thrust. This net thrust coefficient is about 0.3 at ramjet mode and decreases to about 0.1 at scramjet mode. The vertical force coefficient is between 0.2 and 0.3 except Ma 5.5, at which point the combustor operation mode switches from ramjet to scramjet.

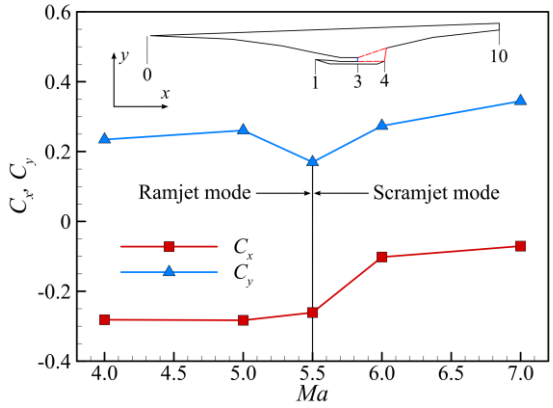

Fig 14. Horizontal and vertical force coefficient at different Mach number

4. Conclusions

A multi-fidelity simulation method is developed based on the implement of a quasi-one dimensional combustor model into commercial solver. This multi-fidelity simulation method is used to analyze external and internal flow physics of the hypersonic vehicle in this paper. The results indicate that:

A multi-fidelity simulation method characterised with high-level fidelity numerical analysis of inlet and nozzle components and low-level fidelity numerical analysis of combustor is developed based on the user-defined function in commercial solver. According to the validation with directed connect wind tunnel tests, the static pressure distribution along the flowpath agrees well with experimental data, which indicates that this simulation method can be used to study the flow physics in hypersonic propulsion system with low cost.

This multi-fidelity simulation method can realize the integration analysis of external and internal flow physics of hypersonic propulsion system at design and off-design points. The results from design point indicate that the combustor operation condition varies with fuel equivalence ratio and it operates at scramjet mode until φ=0.60. The horizontal force increases with fuel equivalence ratio, the thrust balance is achieved at φ=0.35.

The results from off-design points indicate that the combustor operates in ramjet mode from Ma 4.0 to Ma 5.5 and then switches to scramjet mode. The static pressure, temperature and Mach number distribution along the combustor is different between ramjet and scramjet modes which results in net thrust produced by the propulsion system. The net thrust is positive during the whole flight regime between Ma 4-7, and the horizontal force coefficient is about 0.3 at ramjet mode and then decreases to 0.1 at scramjet mode.

Acknowledgments

The authors thanks for the supported from the Fundamental Research Funds for the Central Universities (No.NS20220024) and the National Natural Science Foundation of China (No.11772155).

References

1. Walker, B., Kennedy, K., Mikkeison, C.: US army hypersonic scramjet propelled missile technology program. AIAA Paper, 2006-7927,2006.
2. Heiser, W.H., Pratt, D.T., Daley, D. et al: Hypersonic airbreathing propulsion. Washington DC, AIAA Paper Education Series,1994.

3. Yuan, H.C., Liu, J., Zhang, J.S., et al: The design and validation of over/under turbine-based combined cycle inlet. Aerospace Science and Technology,105(2020)105960.
4. Wang, Y.H., Song, W.Y.: Experimental investigation of influence factors on flame holding in a supersonic combustor. Aerospace Science and Technology,85(2019)180-186.
5. Yu, K.K., Xu, J.L, Lv, Z. et al: Inverse design methodology on a single expansion ramp nozzle for scramjets. Aerospace Science and Technology, 92(2019)9-19.
6. Vu, L.N., Wilson, D.: Quasi-one-dimensional scramjet combustor flow solver using the numerical propulsion system simulation. 2018 Joint Propulsion Conference, Cincinnati, Ohio, 2018.
7. Cao, R.F., Lu, Y., Yu, D.R., et al: Study on influencing factors of combustion mode transition boundary for a scramjet engine based on one-dimensional model. Aerospace Science and Technology,96(2020)105590.
8. Tian, L., Chen, L.H., Chen, Q., Li, F., Chang, X.Y.: Quasi-one-dimensional multimodes analysis for dual-mode scramjet[J]. Journal of Propulsion and Power, 30(6)(2014) 1559-1567.
9. Lytle J .: Multi-fidelity simulations of air breathing propulsion systems. 42nd AIAA/ASME/SAE/ ASEE Joint Propulsion Conference & Exhibit, Sacramento, California, 2006.
10. Smart, M. K.: Scramjets. The Aeronautical Journal, 111(1124) (2007) 605–619.
11. Shapiro, A. H., and Shapiro, R. E. The dynamics and thermodynamics of compressible fluid flow, Volume 1. Wiley, 1953.
12. Bussing, R.T.A., Murman, E.M.: A one-dimensional unsteady model of dual mode scramjet operation. AIAA paper,1983-0422,1983.
13. Liu J.H., Ling, W.H., Liu, X.Z., et al: A quasi-one dimensional unsteady numerical analysis of supersonic combustor performance. Journal of Propulsion Technology. 19(1)(1998) 1-6. (in Chinese)
14. Wang, L.: The numerical simulation of the combustor of scramjet. Northwestern Polytechnical University, Xi'an, 2011. (in Chinese)
15. Billig, F.S.: Research on supersonic combustion. Journal of Propulsion and Power. 9 (4)(1993) 499-514.
16. Jiang, J., Chu, M., Xu, X.: A quasi-one-dimensional method for prediction of dual mode scramjet combustor performance. Journal of propulsion technology. 34(6)(2013)802-808.
17. Kim, H., Liou, M.S.: Flow simulation of N2B hybrid wing body configuration. in 50th AIAA Aerospace Sciences Meeting including the New Horizons Forum and Aerospace Exposition, Nashville, Tennessee, 2012.
18. Vijayakumar, N., Wilson, D.R., Lu, F.K.: Multifidelity simulation of a dual mode scramjet compression system using coupled NPSS and FLUENT codes. 50th AIAA/ASME/SAE/ASEE Joint Propulsion Conference, Cleveland, Ohio, 2014.
19. Connolly, B.J., Krouse,C., Musgrove, G.O.: Implementing a dual-mode scramjet combustor model in NPSS. AIAA Propulsion and Energy Forum,2021.
20. Riggins, D., Tackett, R., Taylor, T.: Thermodynamic analysis of dual-mode scramjet engine operation and performance. AIAA,2006-8059,2006.
21. Anderson J.D.: Computational Fluid Dynamics, McGraw-Hill Science,2010.
22. Baurle, R.A., Gafney, R.L.: Extraction of one-dimensional flow properties from multidimensional data sets. Journal of Propulsion and Power. 24(4)(2008) 704-714.
23. Le, D.B., Goyne, C.P., Krauss, R.H. et al.: Experimental study of a dual-mode scramjet isolator. Journal of Propulsion and Power, 24(5)(2008)1050-1057.
24. Shi, W., Chang, J.T., Zhang, J.L, et al. Numerical investigation on the forced oscillation of shock train in hypersonic inlet with translating cowl. Aerospace Science and Technology, 87(2019)311-322.